Journal of Molecular Catalysis A: Chemical 325 (2010) 98–104

Contents lists available at ScienceDirect

Journal of Molecular Catalysis A: Chemical

journal homepage: www.elsevier.com/locate/molcata

Molecular and dissociative adsorption of water at low-index V_2O_5 surfaces: DFT studies using cluster surface models

P. Hejduk, M. Szaleniec, M. Witko*

Institute of Catalysis and Surface Chemistry, Polish Academy of Sciences, Niezapominajek 8, 30-239 Cracow, Poland

ARTICLE INFO

Article history:
Received 10 February 2010
Received in revised form 8 April 2010
Accepted 9 April 2010
Available online 5 May 2010

Keywords:
Water adsorption
Water dissociation
V_2O_5
DFT
Cluster approach

ABSTRACT

The adsorption of water in both the molecular and dissociative manners at low-index (0 1 0), (1 0 0) and (0 0 1) surfaces of V_2O_5 is examined by DFT methods using an embedded cluster model approach.

The calculations showed that on saturated basal net planes ((0 1 0)V_2O_5), water is stabilized only in molecular form as a result of weak electrostatic interactions, and it may migrate through the surface. At unsaturated side planes ((1 0 0) and (0 0 1) surfaces), both the molecular and dissociative adsorption of water is possible. Molecular stabilization takes place at V centres via coordinative covalent bonds. On the (0 0 1) surface, dissociative adsorption is associated with a moderate energy barrier near bridging oxygen centres and with a very low barrier close to bridging oxygen sites connected to V atoms from different "valley"-like atomic layers. On the (1 0 0) net plane, water undergoes dissociation near the singly and doubly coordinated oxygen sites, although the process is probable only close to the twofold coordinated centre because proximity to vanadyl oxygen sites is accompanied by a high energy barrier.

1. Introduction

Surface hydroxylation plays an important role in many catalytic processes of environmental significance, such as the reduction of NO_x to molecular nitrogen with pre-adsorbed NH_3 (SCR) [1–21] and the selective oxidation of hydrocarbons on V_2O_5-based catalysts. The proposed mechanisms postulate that NH_3 is activated at surface Brönsted acidic sites (surface OH groups) and that the basal (0 1 0) plane is responsible for this step. The basal plane is also thought to take part in the activation of hydrocarbons through C–H splitting.

Surface acidic sites may be formed either as the result of water dissociation at the surface or due to surface reduction by atomic hydrogen. In the first case, two OH groups are created, one bonded to the metallic centre and the second through stabilization of H by the surface oxygen. In the second case, hydrogen becomes adsorbed at any surface O centres, and stable surface OH groups are formed.

Moreover, in many catalytic reactions, the surface of the catalyst is exposed to ambient conditions, where interaction with water is one of the most important aspects of the process and may substantially influence the properties of the catalyst. On one hand, water molecules may compete with the reacting molecule for active sites and thus block them. On the other hand, the catalyst surface may become hydroxylated as a result of the dissociative adsorption of water. Surface hydroxyl groups that are created in this way may serve as active sites in other steps of the catalytic process. The localization of such centres is still a matter of controversy. In the case of vanadia-based catalysts, Miyamoto and Inomata [22–25] suggested their appearance at the basal (0 1 0) surface, whereas Gasior et al. [26] argued that side planes host the OH groups. The existence of Brönsted acidic sites at the unsaturated side (1 0 0) and (0 0 1) faces of vanadia was also postulated by Anderson [27], who showed that these surfaces are full of hydroxyl groups and therefore are responsible for dissociative water adsorption. In addition, Ozkan [28–30] also put forward the hypothesis that V_2O_5 side planes are covered by OH groups and therefore serve as active faces in the SCR process. Yin et al. [31] studied water adsorption on a saturated basal (0 1 0)V_2O_5 surface and simulated its possible dissociation, which led to hydroxylation of this surface. The conclusions were that water only weakly interacts with the basal surface and does not undergo dissociation, so the surface cannot become hydroxylated during such a process. The hypothetical occurrence of the OH groups on the side planes of V_2O_5 was recently supported by calculations of Goclon et al. [32]. The hydrogen adsorption energies of calculated for side planes occurred to be associated with higher exothermic effects than those obtained for the basal (0 1 0) net plane.

In catalytic processes, water is almost always both a reactant and a product. Sometimes it is a by-product, as in oxidative hydrocarbon dehydrogenation, where water formation is a driving force.

Abbreviations: DFT, density functional theory; $E^{ads}(H_2O)$, the energy of water adsorption in a molecular manner; E^{ads}_{diss}, the energy of water adsorption in a dissociative manner; $E^{bar}_{diss}(H_2O)$, the energy barrier of the water dissociation process; PES, potential energy surface; SCR, selective catalytic reduction.

* Corresponding author. Fax: +48 12 4251923.
E-mail addresses: ncwitko@cyf-kr.edu.pl, ncwitko@cyfronet.pl (M. Witko).

1381-1169/$ – see front matter © 2010 Elsevier B.V. All rights reserved.
doi:10.1016/j.molcata.2010.04.004

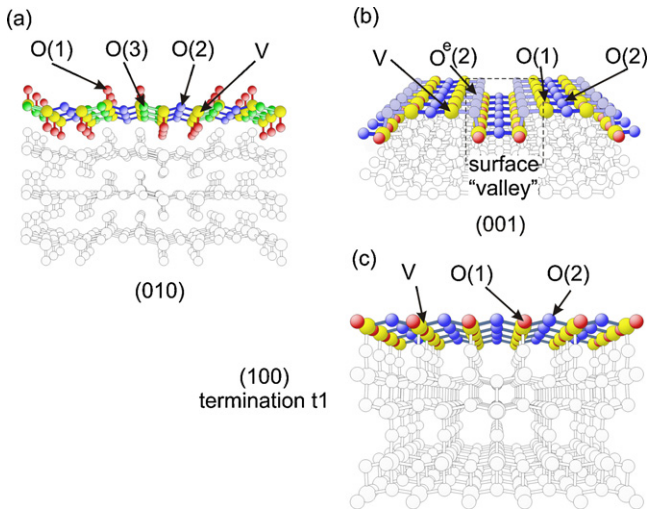

Fig. 1. Three low-index surfaces of vanadium pentoxide: (a) (0 1 0)V_2O_5, (b) (0 0 1)V_2O_5, (c) (1 0 0)V_2O_5 net plane with the most stable "t1" termination [32]. The "t1" termination of (1 0 0)V_2O_5 net plane exposes V atoms and two non-equivalent O atoms: O(1) from a vanadyl group with the V–O(1) bond parallel to the surface and twofold-coordinated O(2) (corresponding to the O(3) sites in the bulk).

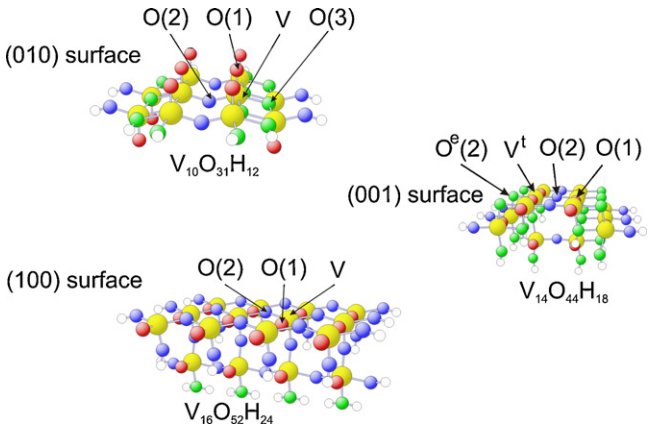

Fig. 2. The surface cluster models for low-index V_2O_5 surfaces. All discussed oxygen and vanadium centres are labelled.

To summarize, the interaction of water with the catalyst surface is one of the most important subjects of study. In the case of vanadia catalysts, it should also be noted that side surfaces contribute up to 15% of the V_2O_5 crystallite structure [33]. This indicates that in addition to the basal plane, these surfaces might also be important in catalytic processes.

In the present paper, the molecular and dissociative adsorption of water at three low-index surfaces of a V_2O_5 catalyst was investigated. A description of the methodology and the surface models is followed by the results of calculations performed for both molecular and dissociative water adsorption. Vibration analyses carried out on the surface species are also discussed. A paragraph that compares water adsorption at the three studied net planes concludes the paper.

2. Computational methods

The vanadium pentoxide crystal is characterized by orthorhombic symmetry with the D_{2h}-P_{mmn} space group and unit cell parameters defined as $a = 11.51$ Å, $b = 4.37$ Å and $c = 3.56$ Å [34,35]. Its structure can be discussed in terms of a building unit of distorted octahedral form with V–O bond distances that vary between very short (1.58 Å, vanadyl groups) and very long (2.79 Å, van der Waals type bonding). Three possible low-index surfaces, (0 1 0), (0 0 1) and (1 0 0), are represented in Fig. 1.

At the saturated basal (0 1 0) surface (Fig. 1a), one can identify vanadium and three structurally different oxygen centres: vanadyl oxygen atoms O(1) singly coordinated to the vanadium atom and two bridging oxygen sites, doubly O(2) and triply O(3) coordinated to two and three vanadium centres, respectively. The side (0 0 1) surface (Fig. 1b), which is composed of "valley"- and "hill"-like regions, is characterized by the existence of coordinatively unsaturated vanadium atoms and three structurally different oxygen sites that lie in plane: vanadyl oxygen O(1) and two bridging oxygen atoms O(2) or $O^e(2)$ (the second connected to V from a different atomic layer and positioned on the edge of the "valley"-like region) bonded to two vanadium atoms. At the flat, most stable termination of the side (1 0 0) surface (Fig. 1c) [33], unsaturated V centres as well as singly O(1)- and double O(2)-coordinated oxygen sites are present. Additionally, all sites are in plane.

To model different low-index V_2O_5 surfaces, the following clusters were chosen: $V_{10}O_{31}H_{12}$, $V_{16}O_{52}H_{24}$ and $V_{14}O_{44}H_{18}$ for the (0 1 0), (1 0 0) and (0 0 1) net planes [36], respectively (see Fig. 2).

Many possible initial geometries for water adsorption were tested. The water molecule was placed parallel as well as perpendicular to the surface, with its H or O atoms pointing toward the surface. The dissociation energy barriers of pre-adsorbed water molecules were approximated by relaxed scans of the potential energy surface (PES) along the O–H. . .O reaction coordinate. The approximated activation barriers were obtained from the differences between respective maximum energies of the PES scans and initial energies of the reactants without further optimization of the transition states.

The electronic structure of the clusters was determined by an *ab initio* density functional theory (DFT) approach, where the Kohn–Sham orbitals were represented by a linear combination of atomic orbitals (LCAO) applying all electron DZVP basis sets of contracted Gaussians obtained from atom optimizations [37,38]. A revised version of the Perdew–Burke–Ernzerhof (RPBE) gradient corrected DFT [39,40] was used to describe the electron exchange-correlation potential. The calculations were carried out with the StoBe software package [41]. The geometries of the model clusters were optimized with Broyden–Fletcher–Goldfarb–Shanno (BFGS) algorithm using the criterion of the minimum of the total energy. The optimization was terminated when the energy gradient was less than 0.0001 a.u.

Detailed analysis of the electronic structure of the systems was investigated by means of charge density distributions (Mulliken populations) [42] and Mayer bond orders [43]. The vibration analysis of adsorbed H_2O and OH species was conducted using a harmonic approximation.

Adsorption energy, which accompanied the stabilization of water in molecular form, was calculated according to the equation:

$$E^{ads}(H_2O) = E_{tot}(V_xO_yH_zH_2O) - [E_{tot}(V_xO_yH_z) + E_{tot}(H_2O)]$$

where $E_{tot}(V_xO_yH_zH_2O)$ describes the total energy of the cluster with the adsorbed water molecule, $E_{tot}(V_xO_yH_z)$ is the total energy of the clean cluster and $E_{tot}(H_2O)$ is the total energy of the ground state of H_2O. The energy of the dissociative type of water adsorption was obtained from the formula: $E^{ads}_{diss}(H_2O) = E_{tot}(V_xO_{y-1}H_zOHOH) - [E_{tot}(V_xO_yH_z) + E_{tot}(H_2O)]$ where $E_{tot}(V_xO_{y-1}H_zOHOH)$ denotes the total energy of the cluster with two OH groups (one formed due to hydrogen stabilization at the surface oxygen and the second by bonding of a hydroxyl to the nearest vanadium site, where both O and OH species originate from H_2O).

Table 1
Adsorption energies $E^{ads}(H_2O)$ for water stabilized in molecular form at the $(0\,1\,0)V_2O_5$ surface modelled by the $V_{10}O_{31}H_{12}$ cluster. In addition, charges of adsorbed H_2O molecule ($Q(H_2O)$), distance between water molecule and the surface (d (surface–H_2O)), as well as its bond order (p (surface–H_2O)) are given.

Adsorption sites	O(1)	O(2)	O(3)	V
$E^{ads}(H_2O)$ [eV]	−0.16	−0.20	−0.16	−0.15
$Q(H_2O)$	−0.003	0.032	0.023	0.041
d (surface–H_2O)	2.23	2.41	2.94	2.78
p (surface–H_2O)	0.04	0.02	0.01	0.01

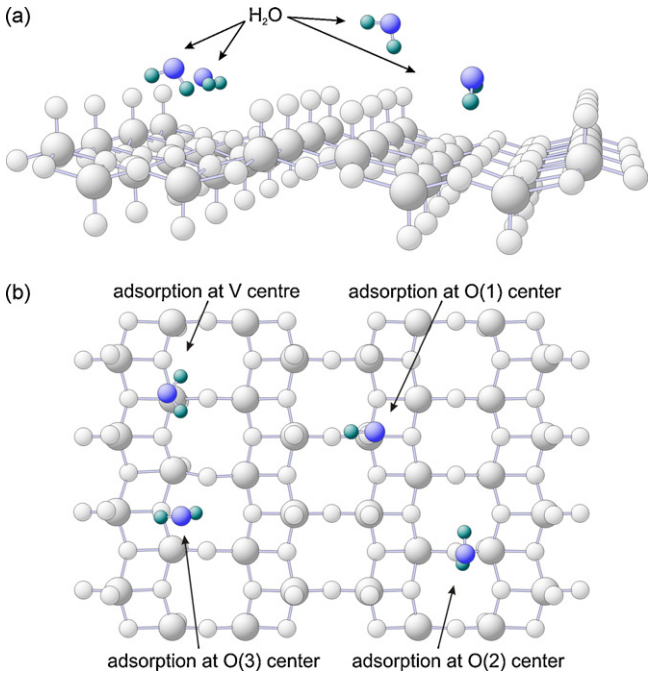

Fig. 3. The geometries of the adsorbed water molecule above oxygen, as well as vanadium active sites at the $(0\,1\,0)V_2O_5$ surface. (a) Perspective view; (b) top view.

3. Results and discussion

3.1. Adsorption and dissociation of water at the $(0\,1\,0)V_2O_5$ surface

Table 1 summarizes $E^{ads}(H_2O)$ energies connected with the adsorption of water in molecular form at the $(0\,1\,0)V_2O_5$ surface mimic by the $V_{10}O_{31}H_{12}$ cluster, charges of the stabilized adsorbate and bond analysis (distances and bond orders) of the system consisting of H_2O and the surface cluster. The final geometries of adsorbed water at the surface of different O and V sites are presented in Fig. 3. It is shown in Table 1 that at the basal $(0\,1\,0)V_2O_5$ surface, water was only weakly stabilized; the adsorption energies were in the range of −0.15 to −0.20 eV. The negligible differences in the adsorption energies connected with different surface sites indicates that the (0 1 0) surface is rather homogeneous from the adsorbate point of view and does not contain any specific adsorption sites. This suggests that water molecules, although stabilized, can move over the (0 1 0) net plane. The migration process is probably restricted only by the low energy barriers.

In local adsorption minima, the surface–H_2O distances are long (2.2–2.9 Å), and bond orders are close to zero. Moreover, from the results of Mulliken population analysis, it is clear that no electron transfer between H_2O molecules and the catalyst surface occurs, irrespective of the adsorption site. As a result, no chemical bond is created and adsorbed H_2O molecules remain neutral. The neutrality of adsorbed H_2O, its final geometry and low adsorption energies

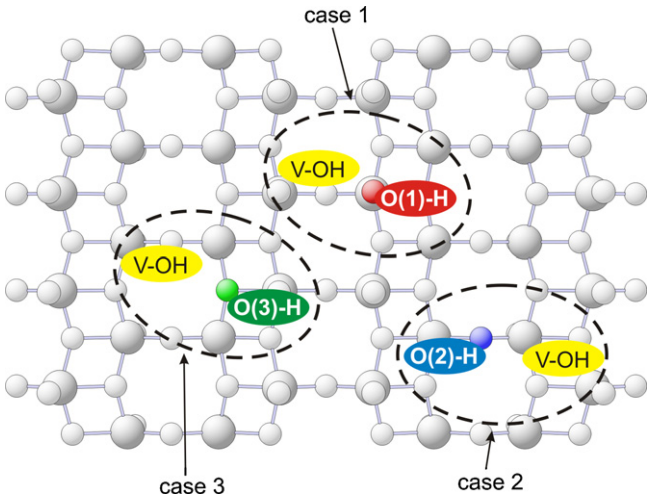

Fig. 4. Scheme view of the studied cases of water molecule dissociation at the $(0\,1\,0)V_2O_5$ surface as modelled by the $V_{10}O_{31}H_{12}$ cluster. V–OH denotes a hydroxyl group (originating from the H_2O molecule) created at the surface V centre, and O(X)–H denotes a second OH group formed from the second H atom (from the H_2O molecule) and surface O(X) atom (X = 1, 2, 3).

confirm the physical (electrostatic) type of H_2O stabilization at the $(0\,1\,0)V_2O_5$ surface. Such electrostatic interaction may be explained by a negative electrostatic potential above the whole basal surface [36], which attracts the water molecule through positively charged hydrogen atoms.

The possible dissociation of water molecules at the $(0\,1\,0)V_2O_5$ surface was also investigated assuming formation of the two adjacent OH groups bonded to the surface in the following manners (Fig. 4):

(1) OH–V and O(1)H (where OH and H come from water; OH is bonded to the V centre, whereas H is bonded to the O(1) site).
(2) OH–V and O(2)H (where OH and H come from water; OH is bonded to the V centre, whereas H is bonded to the O(2) site).
(3) OH–V and O(3)H (where OH and H come from water; OH is bonded to the V centre, whereas H is bonded to the O(3) site).

The calculated adsorption energies connected with water dissociation $E^{ads}_{diss}(H_2O)$ are displayed in the first part of Table 2. For cases 1 and 3, the energy values were positive (1.20 and 1.25 eV), indicating that the studied processes are energetically unfavourable, which means that water dissociation with the involvement of O(1) and O(3) surface sites will not take place. In case 2, from the thermodynamic point of view, water may undergo dissociation (a negative value of (−0.20 eV)); however, geometry optimization led to a system composed of water molecules and the cluster. More-

Table 2
Adsorption energies $E^{ads}_{diss}(H_2O)$ for water stabilized in a dissociative manner and energy barriers $E^{bar}_{diss}(H_2O)$ of the dissociation processes for the studied cases at the (0 1 0), (0 0 1) and (1 0 0)V_2O_5 surfaces (see Sections 3.1–3.3 and Figs. 2, 4 and 6).

$(0\,1\,0)V_2O_5$ surface				
Case	1	2	3	–
$E^{ads}_{diss}(H_2O)$ [eV]	1.20	−0.20	1.25	–
$(0\,0\,1)V_2O_5$ surface				
Case	1	2	3	4
$E^{ads}_{diss}(H_2O)$ [eV]	−0.98	−0.78	−1.27	−0.27
$E^{bar}_{diss}(H_2O)$ [eV]	0.08	0.47	–	–
$(1\,0\,0)V_2O_5$ surface				
Case	1	2	3	–
$E^{ads}_{diss}(H_2O)$ [eV]	−0.89	−0.56	0.14	–
$E^{bar}_{diss}(H_2O)$ [eV]	0.04	0.89	–	–

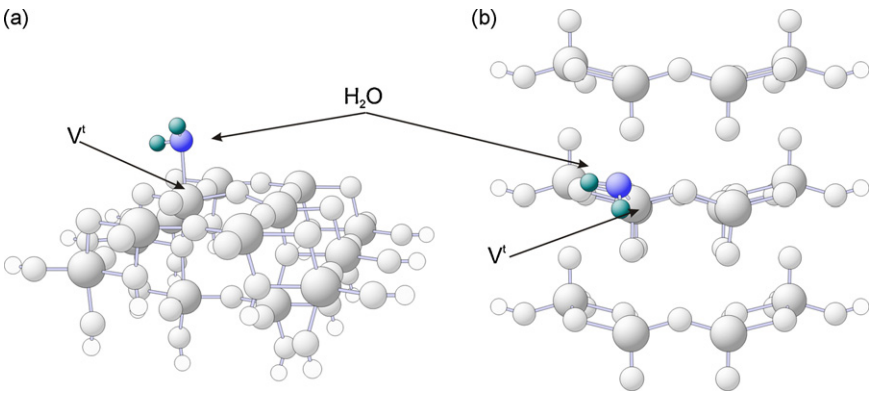

Fig. 5. The geometries of the adsorbed water molecule above oxygen, as well as the vanadium active sites at the (0 0 1)V_2O_5 surface. (a) Perspective view; (b) top view.

Table 3
Adsorption energies $E^{ads}(H_2O)$ for water stabilized in molecular form at the (0 0 1)V_2O_5 surface modelled by the $V_{14}O_{44}H_{18}$ cluster as well as at the (1 0 0)V_2O_5 surface modelled by the $V_{16}O_{52}H_{24}$ cluster. In addition, charge of adsorbed H_2O molecule (Q (H_2O)), distance between water molecule and the surface (d (surface–H_2O)), as well as its bond order (p (surface–H_2O)) are given.

Surface	(0 0 1)V_2O_5	(1 0 0)V_2O_5
$E^{ads}_{diss}(H_2O)$ [eV]	−0.71	−0.56
Q (H_2O)	0.20	0.19
d ($V_{surface}$–OH_2)	2.2	2.3
p ($V_{surface}$–OH_2)	0.35	0.35

over, we could not detect any energy barrier that would kinetically stabilize the existence of two hydroxyl groups and prevent the reconstitution of molecular water. Our results are consistent with experiments where a higher stability of molecular over dissociated water on the V_2O_5 (0 1 0) surface was also found [44,45].

From these investigations, we can conclude that due to the fully saturated character of the V–O bonds at the basal (0 1 0)V_2O_5 surface, water becomes stabilized in molecular form and no water dissociation takes place. This is consistent with previous theoretical studies [27,31] and experimental observations by Haber and co-workers [26].

3.2. Adsorption and dissociation of water at the (0 0 1)V_2O_5 surface

The results of calculations carried out on the process of water adsorption in molecular form at side (0 0 1)V_2O_5 surface sites are summarized in Table 3. One negative value of the adsorption energy $E^{ads}(H_2O)$ (−0.71 eV) indicated that water is stabilized in a molecular manner only close to the vanadium site on the catalyst surface. The final geometry, with H_2O directly bound at the undercoordinated vanadium cation V^t, is plotted in Fig. 5. The formed V^t–OH_2 bond had a bond order equal to 0.35 and a bond distance of 2.2 Å. The Mulliken population showed (Table 3) that the total charge of the water molecule was +0.2, which confirmed the existence of a bonding interaction that originates from shifting of the lone electron pair from the O^{water} atoms toward the empty vanadium 3d orbitals of the surface V^t cation.

The interaction of water with oxygen sites present at the (0 0 1)V_2O_5 surface resulted in dissociative adsorption and led to the formation of two adjacent OH groups. The following cases of water dissociation, which result in the formation of two adjacent OH groups coordinated in the fashions listed below, were also investigated (Fig. 6):

(1) OH–V^t and O^e(2)H (where OH and H come from water; OH is bonded to the V^t centre, whereas H is bonded to the O^e(2) site).

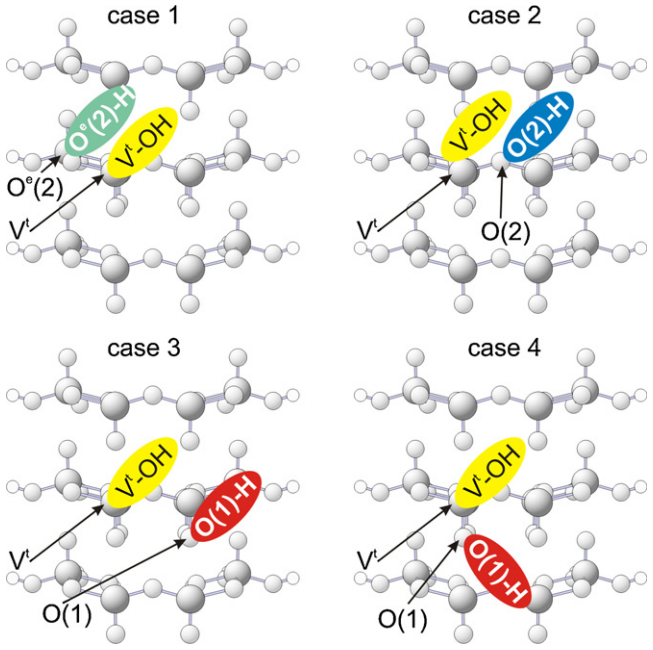

Fig. 6. Scheme view of the studied cases of water adsorption in a dissociative manner at the (0 0 1)V_2O_5 surface as modelled by the $V_{14}O_{44}H_{18}$ cluster. V–OH denotes a hydroxyl group (originating from the H_2O molecule) created at the surface V centre, and O(X)–H denotes a second OH group formed by the second H atom (from H_2O molecule) and surface O(X) atom (X = 1, 2, 2^e).

(2) OH–V^t and O (2)H (where OH and H come from water; OH is bonded to the V^t centre, whereas H is bonded to the O(2) site).
(3) OH–V^t and O(1)H (where OH and H come from water; OH is bonded to the V^t centre, whereas H is bonded to the O(1) site not connected to V^t).
(4) OH–V^t and O(1)H (where OH and H come from water; OH is bonded to the V^t centre, whereas H is bonded to the O(1) site directly connected to V^t).

The results of the calculations can be found in Table 2 (part 2), where the energies and barriers associated with the adsorption of water in a dissociative fashion are listed. The energies $E^{ads}_{diss}(H_2O)$ for all of the studied cases were negative, which implies that dissociation of the H_2O molecule is possible. Moreover, the values of $E^{ads}_{diss}(H_2O)$ −0.98/−0.78/−1.27 eV for cases 1, 2 and 3, respectively, were lower than the value connected with molecular water adsorption (−0.71 eV) at the V^t cation. This indicates that the adsorption of products arising from water dissociation (H + OH leading to 2OH) affords a more stable system than the system in which water is adsorbed in molecular form. Completely different behaviour was

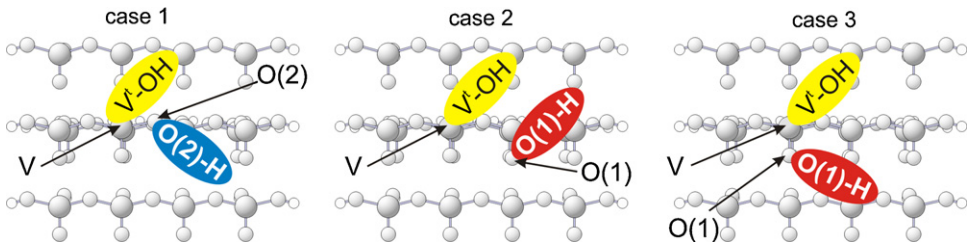

Fig. 7. Scheme view of the studied cases of dissociation of water molecules at the (1 0 0)V_2O_5 surface as modelled by the $V_{16}O_{52}H_{24}$ cluster. V–OH denotes the hydroxyl group (originating from the H_2O molecule) created at the surface V centre, and O(X)–H denotes the second OH group formed by the second H atom (from H_2O molecule) and surface O(X) atom (X = 1, 2).

observed in the last case, where the value $E_{diss}^{ads}(H_2O)$ (−0.27 eV) was higher than the $E^{ads}(H_2O)$ energy. In this case, a system with two hydroxyl groups, although possible, was less stable that the system with water adsorbed as a molecule; this will probably not occur in a real system.

Knowing the possible final configurations and adsorption energies required for the molecular and dissociative processes of water adsorption ($E^{ads}(H_2O)$ and $E_{diss}^{ads}(H_2O)$) at the (0 0 1)V_2O_5 surface, the energy barriers of the dissociation processes $E_{diss}^{bar}(H_2O)$ were calculated. The calculations were performed only for cases 1 and 2, as the reaction path leading to final configuration 3 was neglected due to the fact that the H atom from the H_2O molecule must come across the O(2) site during its possible migration and will become stabilized there. The path resulting in final configuration 4 was not taken into consideration due to the energetic reasons mentioned above.

The calculated energy barriers connected with water dissociation $E_{diss}^{bar}(H_2O)$ (see Table 2) were equal to 0.08/0.47 eV for cases 1 and 2, respectively. Such values indicate that water dissociation leading to configuration 1 is a spontaneous process (negligible energy barrier), whereas dissociation leading to configuration 2 is less likely, but still possible.

To summarize, we conclude that at the (0 0 1)V_2O_5 side surface, water adsorbs in both molecular and dissociative manners. Molecular adsorption takes place at the metallic V^t centre, whereas a dissociative pathway is more favourable near doubly coordinated edging $O^e(2)$ oxygen atoms. In the last case, two hydroxyl surface groups are created; the first where OH (from H_2O), adsorbs at vanadium to form V^t–OH, with the second hydroxyl (H from water) stabilized at the surface oxygen $O^e(2)$ to create $O^e(2)$H. The adsorption of water through dissociation leads to a more stable system (−0.89 eV) than molecular adsorption (−0.71 eV).

3.3. Adsorption and dissociation of water at the (1 0 0)V_2O_5 surface

Molecular and dissociative types of water adsorption were also studied for the (1 0 0)V_2O_5 side surface with "t1" termination [33]. The results for the molecular type of adsorption are given in Table 3, which contains adsorption energies $E^{ads}(H_2O)$, Mulliken populations, Mayer bond order analyses and V–O bond distances.

In accordance with observations on the (0 0 1) plane, at (1 0 0) side surfaces, water is stabilized in molecular form directly above the surface V cations. The process is spontaneous and the adsorption energy $E^{ads}(H_2O)$ equalled −0.56 eV. The stabilization, which was weaker than at the (0 0 1) surface, but much stronger than for saturated (0 1 0) surfaces, was due to the coordinative type of bond originating from the interaction the between lone electron pair of O with empty V 3d orbitals. The length of the new O^{water}–$V^{surface}$ bond was 2.3 Å and its bond order was 0.35. Electron transfer from water to the surface led to a partial charge on the water molecule of +0.19.

In a similar fashion to (0 0 1) side surfaces, the interaction of water with oxygen sites present at the (1 0 0)V_2O_5 surface resulted in a dissociative type of adsorption and led to the formation of two of the following adjacent OH groups (Fig. 7):

(1) OH–V and O(2)H (where OH and H come from water; OH is bonded to the V centre, whereas H is bonded to the O(2) site).
(2) OH–V and O(1)H (where OH and H come from water; OH is bonded to the V centre, whereas H is bonded to the O(1) site).
(3) OH–V and O(1)H (where OH and H come from water; OH is bonded to the V centre, whereas H is bonded to the O(1) site connected with the first V–OH).

The results of these calculations can be found in Table 2. For final configurations 1 and 2, energies connected with the dissociative adsorption were negative, which indicates that such processes are possible. The adsorption energy $E_{diss}^{ads}(H_2O)$ for case 1 (−0.89 eV) was lower than the energy related to molecular adsorption (−0.56 eV) of water at the vanadium cation. That is, the system where water adsorbs dissociatively was more stable than the system where molecular water was stabilized. This suggests that water molecules will undergo dissociation near site O(2). The $E_{diss}^{ads}(H_2O)$ energy for configuration 2 was equal to the $E^{ads}(H_2O)$ energy, which implies that near O(1) sites, water may be stabilized according to both mechanisms, molecular and dissociative. Adsorption that proceeds through case 3 leads to an unstable system.

Understanding the possible stable surface configurations of the two adjacent OH groups created due to water dissociation and the energies connected with these processes allows one to examine the dissociation energy barriers $E_{diss}^{bar}(H_2O)$. The calculations were carried out only for cases leading to final configurations 1 and 2. The energy barriers for dissociation resulting in final configurations 1 and 2 were equal to 0.04 and 0.89 eV, respectively, which indicates that processes occurring near a bridging sites O(2) are spontaneous, whereas those close to vanadyl oxygen O(1) centres are energetically demanding.

3.4. Vibration analysis

In the following section, vibration analyses for the water molecules adsorbed in molecular or dissociative forms are presented and compared with the experimental data. Experimentally [46,47], the OH stretching frequencies of the hydroxyl groups in a water molecule are reported to be 3657, 3756 and 1595 cm^{-1} for symmetric stretching (SS), asymmetric stretching (AS) and bending (B) modes, respectively. The analogous frequency for surface OH species localized at vanadium cations (V–OH) in V_2O_5 [48,3] is 3659 cm^{-1}.

The calculated frequencies are listed in Table 4. The results of vibration analysis for the (0 1 0) surface can be compared only with the experimental frequencies of the isolated H_2O molecule because no dissociation was observed at this net plane. Theoretical

Table 4
Calculated frequencies [cm^{-1}] of symmetric (SS) and asymmetric (AS) stretching modes of OH groups from the H_2O molecule; bending modes (B) of H_2O molecules and stretching mode of surface OH groups at the V_2O_5 surfaces [60–63]; (Δ) the shifts of the theoretical frequencies with respect to the experimental values.

Surface (0 1 0) modes [cm^{-1}]	O(1)	O(2)	O(3)	V
SS (Δ)	3671 (+14)	3668 (+11)	3692 (+35)	3675 (+18)
AS (Δ)	3778 (+22)	3778 (+22)	3805 (+49)	3780 (+24)
B (Δ)	1611 (+16)	1582 (−13)	1589 (−6)	1583 (−12)

Surface (0 0 1) modes [cm^{-1}]	Case 1		Case 2		
	O(2)H	OH	$O^e(2)$	OH	V
SS (Δ)	–	–	–	–	3510 (−147)
B (Δ)	–	–	–	–	1552 (−43)
$O–H^{surface}$ (Δ)	3611 (−48)	3651 (−8)	3662 (+3)	3553 (−116)	–

Surface (1 0 0) modes [cm^{-1}]	Case 1		Case 2		
	O(2)H	OH	O(1)H	OH	V
SS (Δ)	–	–	–	–	3617 (−40)
B (Δ)	–	–	–	–	1514 (−81)
$O–H^{surface}$ (Δ)	3489 (−170)	3619 (−40)	3443 (−216)	3662 (+3)	–

wavenumbers of both the symmetric and asymmetric stretching OH modes were in good agreement with experimental values [46,47]. Small shifts confirmed that water molecules interact with the (0 1 0) net plane very weakly, which is in agreement with energetic data previously reported (see Table 1).

The situation was different in the case of molecular water adsorption at both side (0 0 1) and (1 0 0) surfaces, where H_2O is linked to the surface through V–O coordination. Here, the shifts of the IR frequencies were larger (up to 147 cm^{-1}), not so close to the experimental values, although confirming the existence of water species stabilized at surface vanadium cations. It is also important to underline that the experimental spectrum comes from the crystals with predominant (app. 85% [33]) exposition of (0 1 0) plane. As a result the biggest share of IR spectrum should also come from the (0 1 0)V_2O_5–H_2O interactions. As a consequence the discrepancies between calculated frequencies of water adsorbed on the side surfaces and the experimental spectrum are to be expected.

For dissociative water adsorption at the (0 0 1) and (1 0 0) side surfaces, the stretching frequencies of OH groups were between 3443 and 3662 cm^{-1}, depending on the origin of the surface hydroxyl species. The differences in the wavenumbers, which range from +3 to −216 cm^{-1}, depend on the local geometries of the V–OH sites.

In summary, we can conclude that the theoretical values of IR frequencies are in acceptable agreement with the experimental data and confirm the type of adsorption hypothesized for each surface feature. For molecular adsorption, the differences between theoretical and experimental frequencies were small, while for dissociative adsorption, they are bigger and strongly depend on the surface adsorption site. Therefore, IR analysis of V_2O_5 crystallites of different morphologies may be a qualitative method to study the involvement of different surface hydroxyl groups at different surfaces in catalytic processes.

4. Conclusions

The adsorption of water molecules on low-index V_2O_5 surfaces depends on the type of surface and the local geometry of the adsorption site. At saturation basal (0 1 0) net plane water becomes stabilized in molecular form. The adsorption energies are small, indicating the possibility of water migration through the surface. In this case, adsorption is due to the electrostatic interactions between adsorbate and the surface.

The situation is different for (0 0 1) and (1 0 0) side surfaces, where both molecular and dissociative mechanisms of water adsorption may occur. Molecular adsorption takes place at the metallic centre and leads to the formation of a covalent coordinative bond by partial donation of lone pair electrons of O^{H_2O} to empty 3d vanadium orbitals. Water is stabilized dissociatively in the vicinity of oxygen surface sites on the (0 0 1) surface near doubly coordinated edging $O^e(2)$ oxygen atoms, whereas for the (1 0 0) plane, it is stabilized close to doubly coordinated O(2) sites. In both cases, the processes are nearly spontaneous and lead to the formation of two hydroxyl surface groups. In the first case, OH that originates from H_2O adsorbs at the vanadium site, forming V–OH. In the second case, H (from water) is stabilized at the surface oxygen $O^e(2)$ or O(2) sites, creating $O^e(2)$H or O(2)H, respectively. The dissociation of water at both surfaces is also possible near the vanadyl sites, although this process is accompanied by a higher energy barrier than that occurring close to the surface oxygen sites. Analysis of IR frequencies may be used to define the type of surface and type of site where surface OH species are formed and may serve as a fingerprint for the surface reaction. The performed calculations indicated that under ambient conditions, side planes of V_2O_5 catalysts may become hydroxylated and covered by hydroxyl groups, which has been postulated previously [26,27].

Acknowledgements

Financial support by the Polish Ministry of Science and High Education (grant no. N204 024 31/0475) is gratefully acknowledged.

References

[1] B. Grzybowska-Świerkosz, Appl. Catal. A 157 (1997) 263–310.
[2] H. Bosch, F. Janssen, Catal. Today 2 (1988) 369–379.
[3] N.-Y. Topsoe, J. Catal. 128 (1991) 499–511.
[4] Y. Cai, U.S. Ozkan, Appl. Catal. 78 (1991) 241–255.
[5] N.-Y. Topsoe, H. Topsoe, J.A. Dumesic, J. Catal. 151 (1995) 226–240.
[6] J.A. Dumesic, N.-Y. Topsoe, H. Topsoe, Y. Chen, T. Slabiak, J. Catal. 163 (1996) 409–417.
[7] L. Lieti, P. Forzatti, F. Bregani, Ind. Eng. Chem. Res. 35 (1996) 3884–3892.
[8] L. Lietti, J.L. Alemany, P. Forzatti, G. Busca, G. Ramis, E. Giamello, F. Bregani, Catal. Today 29 (1996) 143–148.
[9] B.L. Dufy, H.E. Curry-Hyde, N.W. Cant, P.F. Nelson, J. Phys. Chem. 98 (1994) 7153–7161.
[10] G. Ramis, L. Yi, G. Busca, M. Turco, E. Kotur, R.J. Willey, J. Catal. 157 (1995) 523–535.
[11] S. Hu, T.M. Apple, J. Catal. 158 (1996) 199–204.
[12] L.G. Pinaeva, A.P. Suknev, A.A. Budneva, E.A. Paukshtis, B.S. Balzhinimaev, J. Mol. Catal. A: Chem. 112 (1996) 115–124.
[13] E. Tronconi, L. Lietti, P. Forzatti, S. Malloggi, Chem. Eng. Sci. 51 (1996) 2965–2970.

[14] G. Qi, R.T. Yang, Catal. Lett. 100 (2005) 243–246.
[15] V.I. Parvulescu, P. Grange, B. Delmon, Catal. Today 46 (1998) 233–316.
[16] G. Busca, L. Lietti, G. Ramis, F. Berti, Appl. Catal. B 18 (1998) 1–36.
[17] G.C. Bond, P. Forzatti, J.C. Vedrine, Catal. Today 56 (2000) 329–332.
[18] G. Coudurier, J.C. Vedrine, Catal. Today 56 (2000) 415–430.
[19] M. Calatayud, B. Mguig, C. Minot, Surf. Sci. Rep. 55 (2004) 169–236.
[20] E. Tronconi, I. Nova, C. Ciardelli, D. Chatterjee, M. Weibel, J. Catal. 245 (2007) 1–10.
[21] J.H. Goo, M.F. Irfan, S.D. Kim, S.C. Hong, Chemosphere 67 (2007) 718–723.
[22] M. Inomata, A. Miyamoto, Y. Murakami, J. Catal. 62 (1980) 140–148.
[23] M. Inomata, A. Miyamoto, T. Ui, K. Kobayashi, Y. Murakami, Ind. Eng. Chem. Prod. Res. Dev. 21 (1982) 424–428.
[24] A. Miyamoto, Y. Yamazaki, T. Hattori, M. Inomata, Y. Murakami, J. Catal. 74 (1982) 144–155.
[25] A. Miyamoto, K. Kobayashi, M. Inomata, Y. Murakami, J. Phys. Chem. 86 (1982) 2945–2950.
[26] M. Gasior, J. Haber, T. Machej, T. Czeppe, J. Mol. Catal. 43 (1988) 359–369.
[27] A. Anderson, J. Solid State Chem. 42 (1982) 263–275.
[28] U.S. Ozkan, Y. Cai, M.W. Kumthekar, Appl. Catal. A 96 (1994) 365–381.
[29] U.S. Ozkan, Y. Cai, M.W. Kumthekar, L. Zhang, J. Catal. 142 (1993) 182–197.
[30] U.S. Ozkan, Y. Cai, M.W. Kumthekar, J. Catal. 149 (1994) 390–403.
[31] X. Yin, H. Han, A. Endou, M. Kubo, A. Chatterjee, A. Miyamoto, J. Phys. Chem. B 103 (1999) 3218–3224.
[32] J. Goclon, R. Grybos, M. Witko, J. Hafner, Phys. Rev. B 79 (2009) 0754391–754414.
[33] J. Goclon, R. Gryboś, M. Witko, J. Hafner, J. Phys.: Condens. Matter 21 (2009) 095008.
[34] H.G. Bachman, F.R. Ahmed, W.H. Barnes, Z. Kristallogr. Kristallgeom. Kristallphys. Kristallchem. 115 (1981) 110.
[35] R.W.G. Wyckoff, Crystal Structures, Interscience, Wiley, New York, 1965.
[36] P. Hejduk, M. Witko, K. Hermann, Top. Catal. 52 (2009) 1105–1115.
[37] J.K. Labanowski, J.W. Anzelm (Eds.), Density Functional Methods in Chemistry, Springer, New York, 1991.
[38] N. Godbout, D.R. Salahub, J. Anzelm, E. Wimmer, Can. J. Phys. 70 (1992) 560–571.
[39] J.P. Perdew, K. Burke, M. Ernzerhof, Phys. Rev. Lett. 77 (1996) 3865–3868.
[40] B. Hammer, L.B. Hansen, J.K. Nørskov, Phys. Rev. B 59 (1999) 7413–7421.
[41] StoBe-deMon 2.0, K. Hermann, L.G.M. Pettersson, M.E. Casida, C. Daul, A. Goursot, A. Koester, E. Proynov, A. St-Amant, D.R. Salahub, contributing authors: V. Carravetta, H. Duarte, N. Godbout, J. Guan, C. Jamorski, M. Leboeuf, V. Malkin, O. Malkin, M. Nyberg, L. Pedocchi, F. Sim, L. Triguero, A. Vela, StoBe Software.
[42] R.S. Mulliken, J. Chem. Phys. 23 (1955) 884–887.
[43] I. Mayer, J. Mol. Struct. Theochem. 149 (1987) 81–89.
[44] D. Göbke, Y. Romanyshyn, S. Guimond, J.M. Sturm, H. Kuhlenbeck, J. Döbler, U. Reinhardt, M.V. Ganduglia-Pirovano, J. Sauer, H.-J. Freund, Angew. Chem. 48 (2009) 3695–3698.
[45] J.M. Sturm, D. Göbke, H. Kuhlenbeck, J. Döbler, U. Reinhardt, M.V. Ganduglia-Pirovano, J. Sauerz, H.-J. Freund, Phys. Chem. Chem. Phys. 11 (2009) 3290–3299.
[46] R. Lemus, J. Mol. Spectrosc. 225 (2004) 73–92.
[47] A. Janca, K. Tereszchuk, P.F. Bernath, N.F. Zobov, S.V. Shirin, O.L. Polyansky, J. Tennyson, J. Mol. Spectrosc. 219 (2003) 132–135.
[48] G. Busca, Langmuir 2 (1986) 577–582.